

Dielectric characteristics of low-permittivity silicate using electron beam direct patterning for intermetal dielectric applications

Po-Tsun Liu, T. C. Chang, T. M. Tsai, Z. W. Lin, C. W. Chen, B. C. Chen, and S. M. Sze

Citation: [Applied Physics Letters](#) **83**, 4226 (2003); doi: 10.1063/1.1628401

View online: <http://dx.doi.org/10.1063/1.1628401>

View Table of Contents: <http://scitation.aip.org/content/aip/journal/apl/83/20?ver=pdfcov>

Published by the [AIP Publishing](#)

Articles you may be interested in

[Thermal stability of trimethylsilylated mesoporous silica thin films as the ultralow- k dielectric for copper interconnects](#)

J. Vac. Sci. Technol. B **23**, 2034 (2005); 10.1116/1.2050656

[Surface modified silica mesoporous films as a low dielectric constant intermetal dielectric](#)

J. Appl. Phys. **92**, 3338 (2002); 10.1063/1.1499979

[Synthesis of organically modified mesoporous silica as a low dielectric constant intermetal dielectric](#)

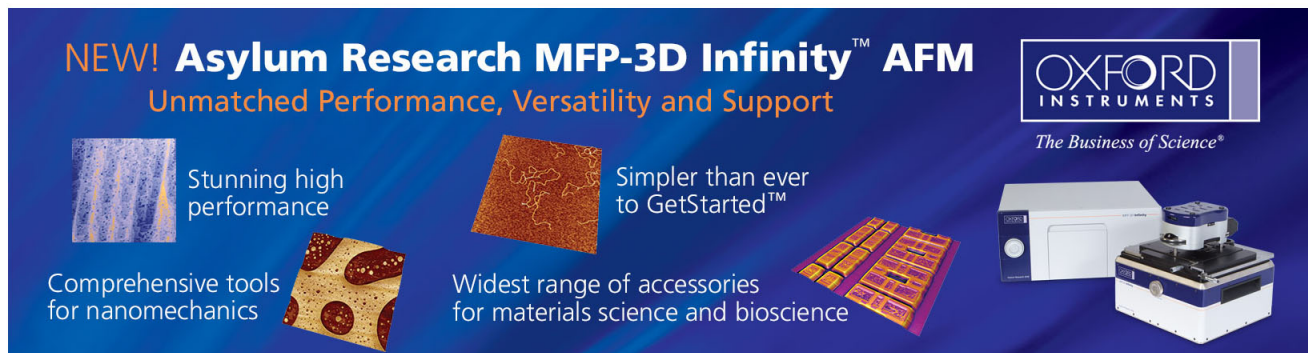
J. Vac. Sci. Technol. B **20**, 2036 (2002); 10.1116/1.1506904

[Direct patterning of photosensitive low-dielectric-constant films using electron-beam lithography](#)

Appl. Phys. Lett. **78**, 2557 (2001); 10.1063/1.1360777

[Surface modified spin-on xerogel films as interlayer dielectrics](#)

J. Vac. Sci. Technol. B **17**, 205 (1999); 10.1116/1.590541

The advertisement features a dark blue background with white and orange text. At the top left, it reads 'NEW! Asylum Research MFP-3D Infinity™ AFM' in large white letters, followed by 'Unmatched Performance, Versatility and Support' in orange. On the right, the Oxford Instruments logo is shown with the tagline 'The Business of Science®'. Below the text are four images: a textured surface, a circular pattern, a grid of small squares, and the AFM instrument itself. Each image is accompanied by a short text description: 'Stunning high performance', 'Simpler than ever to GetStarted™', 'Comprehensive tools for nanomechanics', and 'Widest range of accessories for materials science and bioscience'.

Dielectric characteristics of low-permittivity silicate using electron beam direct patterning for intermetal dielectric applications

Po-Tsun Liu^{a)}

National Nano Device Laboratory, 1001-1 Ta-Hsueh Road, HsinChu 300, Taiwan, Republic of China

T. C. Chang

Department of Physics, Institute of Electro-Optical Engineering, National Sun Yat-Sen University, Taiwan, Republic of China

T. M. Tsai, Z. W. Lin, and C. W. Chen

Institute of Electronics, National Chiao Tung University, Taiwan, Republic of China

B. C. Chen and S. M. Sze

National Nano Device Laboratory, 1001-1 Ta-Hsueh Road, HsinChu 300, Taiwan, Republic of China

(Received 12 May 2003; accepted 22 September 2003)

A direct patterning technology of low-permittivity silicate-based polymer is investigated with electron-beam lithography for multilevel interconnections. The smallest feature size of 60 nm for damascene lines can be directly patterned in the silicate film. In this direct patterning, dielectric regions exposed by electron beam are crosslinked and form desirable patterns, while the others are dissolvable in an aqueous solution containing 2.38% tetramethylammonium hydroxide. With an optimum condition of electron-beam lithography, the electron-beam-irradiated silicate exhibits superior dielectric properties than that of the furnace-cured silicate film, due to minimizing the break of Si-H bonds and moisture uptake. The explanation is in agreement with the analyses of Fourier transform infrared spectroscopy and thermal desorption spectroscopy. © 2003 American Institute of Physics. [DOI: 10.1063/1.1628401]

As feature sizes of integrated circuits reduce beyond 180 nm and enter the sub-100-nm nanoscale fields, signal propagation delay due to parasitic resistance and capacitance between the interconnect lines becomes the predominant component of the overall device signal delay.¹ The crosstalk and power dissipation both also increase with the escalating parasitic capacitance. To address these problems, copper (Cu) damascene technology with low permittivity (low- k)²⁻⁵ intermetal dielectrics (IMD) has been developing for multilevel interconnects. It is necessary to reduce fabrication procedures for the interconnect architecture, especially etch-stop layer, photoresist, and dry-etching processes for damascene technology. Moreover, it is worth noticing that low- k dielectrics are easily degraded during photoresist stripping processes.^{6,7} Direct patterning of low- k dielectrics using electron beam (EB) lithography is a promising choice to simplify process steps and to avoid the damage from photoresist stripping during Cu damascene manufacture.⁸ Although the major drawback of EB lithography is the very small throughput compared to current optical steppers, new ideas on masks and scanning strategies have been developing to resolve the throughput limitation on EB system.⁹⁻¹⁰ In this direct patterning, it was found that several low- k dielectric materials were sensitive to EB exposure. One of them, hydrogen silsesquioxane (HSQ)¹¹ was used as a negative tone electron beam resist,¹² since HSQ did not show only high resolution with a sensitivity comparable to poly(methyl methacrylate) (PMMA) but also a very low edge roughness.¹³ For the EB resist applications, HSQ layers are always stripped after finishing pattern transfer; thereby, dielectric properties of the

HSQ films exposed by EB irradiation are not main factors in the process considerations. On the contrary, for IMD applications, low- k dielectric characteristics such as leakage current and dielectric constant naturally need to be carefully taken into consideration.¹ In this letter, direct patterning of low- k HSQ using EB lithography is proposed as a multilevel interconnect technology. Dielectric characteristics of EB-exposed HSQ films are also investigated for IMD applications.

A nonphotosensitive silicate-based polymer, hydrogen silsesquioxane, was used as an electron sensitive low- k material through this study. HSQ resins diluted in methylisobutyl ketone (MIBK) were spun onto 6-in.- p -type Si wafers at 2000 rpm for 20 s to form 500-nm-thick films. After hot baking at 150 °C on a hot plate for 1 min, EB exposure was carried out according to target pattern layouts by use of a Leica Wepriint200 stepper. The EB energy was 40 kV with beam size 20 nm and the exposure doses were changed from 100 to 700 $\mu\text{C}/\text{cm}^2$. After EB exposure, the HSQ films were developed in an aqueous solution containing 2.38% tetramethylammonium hydroxide (TMAH) for 1 min and rinsed in deionized water for 1 min. For the IMD dielectric investigations, unpatterned HSQ films were fabricated with EB blanketly irradiating on the post-baked HSQ films. Then, the HSQ films were immersed in aforementioned developer TMAH and deionized water. Furnace annealing was finally performed at temperatures between 300 and 350 °C for 60 min in N_2 ambient to remove the residual organic solvent and to enhance the dielectric properties of EB-exposed HSQ films. The control samples were also manufactured for comparison, according to a typical commercial recipe, by baking as-spun HSQ films at 150, 200, and 300 °C for 1 min, re-

^{a)}Electronic mail: ptliu@ndl.gov.tw

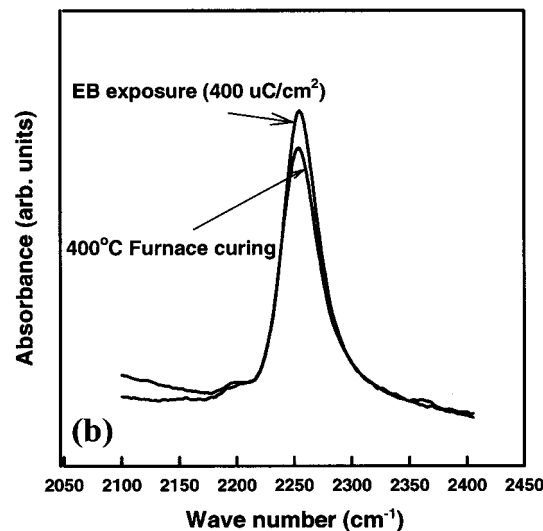
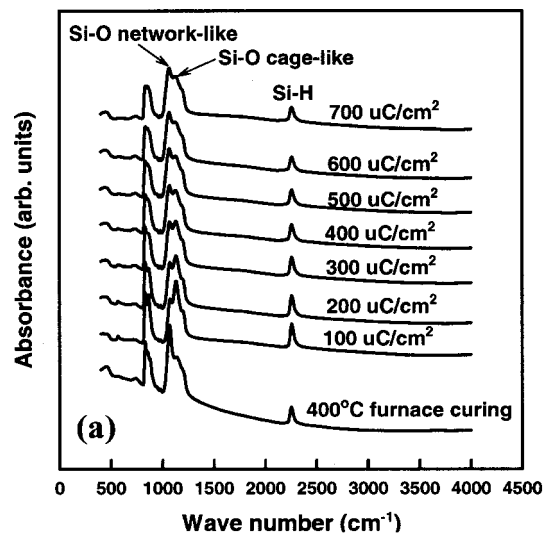


FIG. 1. (a) FTIR spectra of as-baked HSQ films with different doses of EB exposure, ranging from 100 to 700 $\mu\text{C}/\text{cm}^2$. (b) The enlargement of (a), ranging from 2100 to 2400 cm^{-1} , for comparing the EB-exposed HSQ with the furnace-cured HSQ films.

spectively, and followed by thermal curing in a furnace at 400 °C for 60 min under N_2 atmosphere. The chemical structures of all the HSQ films were determined by Fourier transform infrared (FTIR Bio-Red QS300) spectrometry. Electrical measurements were conducted on metal insulator semiconductor (MIS) capacitors. Material analysis using thermal desorption spectroscopy (TDS) was carried out upon heating samples from room temperature to 600 °C at a heating rate of 20 °C/s in vacuum (10^{-5} Pa). In the TDS analysis, m/e (mass-to-charge ratio)=18 peak that is attributed to H_2O was monitored to evaluate dielectric stability of the EB-exposed HSQ films.

FTIR spectra of HSQ films with different doses of EB exposure are shown in Fig. 1(a). In the HSQ film, Si-O bending mode (cage-like vibration at 863 cm^{-1}), Si-O stretching modes (cage-like vibration at near 1130 cm^{-1} , network-like vibration at near 1070 cm^{-1}), and Si-H stretching mode (near 2260 cm^{-1}) are observed. The Si-H group makes the surface of HSQ film hydrophobic and prevents moisture uptake. In addition, the low- k properties of HSQ film can be achieved if the density of Si-H bonding is

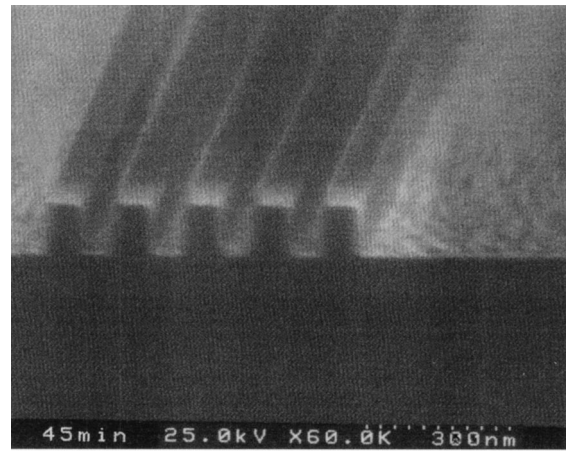
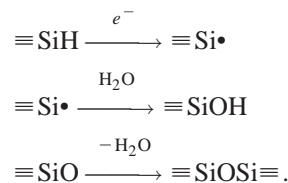


FIG. 2. SEM micrograph of patterned HSQ film with critical dimension of 60 nm.

maintained at a high level.¹⁴ With EB exposure, it is found that the peaks of Si-O stretching modes significantly change. The EB irradiation provides the as-baked HSQ film energy to be crosslinked and transfer the HSQ from cage-like structure to a network-like one. It clearly shows the intensity of Si-O network mode growth at the expense of the intensity of Si-O cage mode with increasing EB exposure doses. Moreover, the intensity of Si-H stretching mode is slightly decreased with increasing EB exposure doses. This observation indicates the structure of HSQ film changes from a cage-like to a stable three-dimensional network structure via the breakage of Si-O cage bonds and Si-H bonds, and subsequently forming Si-O-Si network bonding. The chemical reactions by EB¹² could be simply summarized as follows:



However, an excess of Si-H bonding breakdown will lead to the generation of dangling bonds in HSQ film, resulting in degraded dielectric properties.¹⁴⁻¹⁶ The optimum EB exposure, in this work, was obtained with a minimum dose of 400 $\mu\text{C}/\text{cm}^2$. In comparison with the furnace-cured HSQ film, as shown in Fig. 1(b), the intensity of Si-H bonds in the HSQ film with EB dosage 400 $\mu\text{C}/\text{cm}^2$ is relatively high. This result implies the EB-exposed HSQ could have superior dielectric characteristics than that of the furnace-cured HSQ. Scanning electron microscopy (SEM) micrographs of line patterns are displayed in Fig. 2. Dielectric regions of the HSQ films exposed by EB are crosslinked, while the others without EB exposure maintain gel-like states and are dissolvable in the TMAH aqueous solution, further forming trench patterns. The trench patterns will be suitable for the subsequent fill of Cu damascene lines. Also, Fig. 2 shows a good image selection ratio for the developer TMAH. The dimension with 60 nm for line widths is obtained with an EB dose of 400 $\mu\text{C}/\text{cm}^2$ without using conventional photoresist and dry-etching techniques. Figure 3 shows electrical characteristics of the EB exposed and furnace-cured HSQ films. The inset of Fig. 3 compares the dielectric constant of both

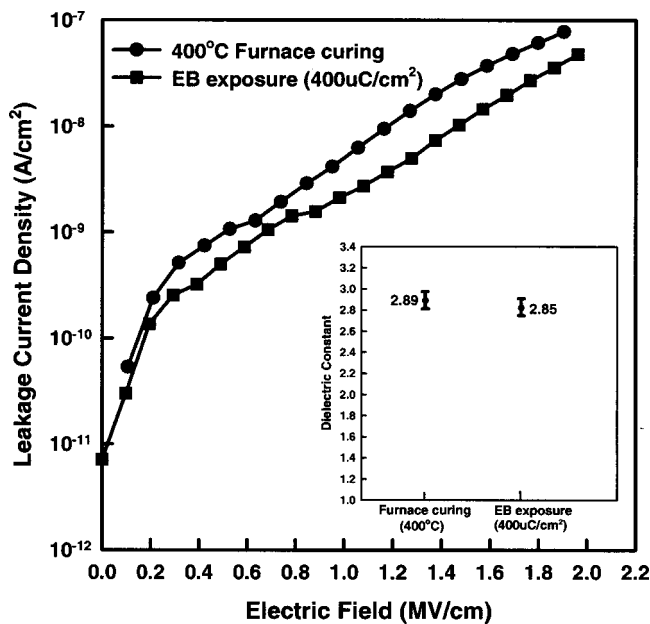


FIG. 3. Leakage current of the EB-exposed and the furnace-cured HSQ films as a function of electric fields. The inset plot compares the dielectric constant of HSQ films between using electron beam exposure and furnace curing.

samples. As can be seen, the leakage current of HSQ film with furnace curing is higher than that of the EB-exposed HSQ film. This phenomenon could be attributed to the fact that typically used furnace curing above 375 °C leads to Si–H bonds being broken,^{14,15} generating dangling bonds in the HSQ film. It is also consistent with the FTIR spectra [Fig. 1(b)] that less Si–H bonds exist in the furnace-cured HSQ compared to the EB-exposed HSQ. These dangling bonds are electrically trap centers and prone to moisture uptake, easily forming leaky paths in HSQ film. In comparison with furnace curing, electron beam exposure uses high-energy electrons rather than heat, to initiate polymerization and crosslinking reactions in the silicate-based polymer. It thereby enhances specific physical and chemical properties, and minimizing the formation of dangling bonds. TDS analysis shown in Fig. 4 surely confirms our inference that the relatively high moisture content is monitored in the furnace-cured HSQ film. The first desorption peak at ~200 °C is attributed to moisture adsorbed at the silicate surface, and the second peak at 400–600 °C is attributed to moisture tightly bonded through Si–OH groups at the internal surface of silicate films.¹⁷ Therefore, the furnace-cured HSQ exhibits inferior dielectric characteristics to that of the EB-exposed HSQ due to relatively high moisture adsorption.

In conclusion, direct patterning of nonphotosensitive low-*k* HSQ has been achieved using EB lithography. In this work the smallest feature size of 60 nm for damascene lines has been demonstrated without using etch-stop layer, photoresist, and dry-etching technologies. The probability of low-*k* degradation can be thereby avoided during these pattern transfer processes. For intermetal dielectric applications, low-*k* characteristics of the HSQ film with EB exposure have been emphasized to explore. With an optimum condition of EB lithography, the EB-exposed HSQ film exhibits superior low-*k* properties than that of the furnace-cured HSQ, due to minimizing the break of Si–H bonds and moisture uptake.

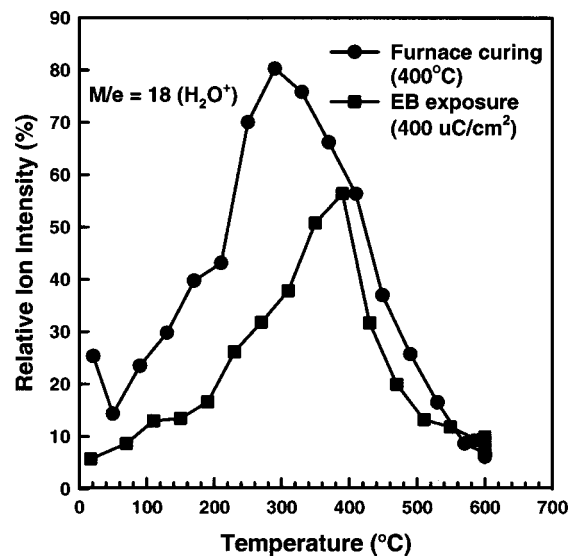


FIG. 4. Temperature dependence of moisture ($m/e = 18$) desorption from HSQ films with electron beam exposure and with furnace curing.

Material analyses including FTIR and TDS have confirmed our explanation, certainly indicating that relatively high intensity of Si–H bonds and low content of moisture are present in the electron-beam-exposed silicate.

This work was performed at Nano Device Laboratories, Taiwan, R.O.C. The authors thank Dr. Fu-Hsiang Ko and Dr. Hsuen-Li Chen at NDJ for assistance in this work. Also, the authors gratefully acknowledge the support from Dr. J. K. Lee, Grace Chen, Eric Tsai, and Joe Chang, at Dow Corning, Taiwan Inc.

¹International Technology Roadmap for Semiconductors (ITRS), Santa Clara, CA, November, 2001.

²K. Postava, T. Yamaguchi, and M. Horie, *Appl. Phys. Lett.* **79**, 2231 (2001).

³A. Mallikarjunan, S. P. Murarka, and T. M. Lu, *Appl. Phys. Lett.* **79**, 1855 (2001).

⁴T. Sugiyama, T. Tai, and T. Sugino, *Appl. Phys. Lett.* **80**, 4214 (2002).

⁵H. J. Lee, E. K. Lin, B. J. Bauer, W. I. Wu, B. K. Hwang, and W. D. Gray, *Appl. Phys. Lett.* **82**, 1084 (2003).

⁶H. C. Liou, J. Duel, V. Finh, Q. Han, P. Sakhivel, and R. Ruffin, *Mater. Res. Soc. Symp. Proc.* **612**, D5.11 (2000).

⁷P. T. Liu, T. C. Chang, Y. S. Mor, C. W. Chen, T. M. Tsai, C. J. Chu, F. M. Pan, and S. M. Sze, *Electrochem. Solid-State Lett.* **5**, G11 (2002).

⁸T. Kikkawa, T. Nagahara, and H. Matsuo, *Appl. Phys. Lett.* **78**, 2557 (2001).

⁹S. D. Berger and J. M. Gibson, *Appl. Phys. Lett.* **57**, 153 (1990).

¹⁰L. R. Harriott, *J. Vac. Sci. Technol. B* **15**, 2130 (1997).

¹¹M. J. Loboda, C. M. Grove, and R. F. Schneider, *J. Electrochem. Soc.* **145**, 2861 (1998).

¹²H. Namatsu, Y. Takahashi, K. Yamazake, T. Yamaguchi, M. Nagase, and K. Kurihara, *J. Vac. Sci. Technol. B* **16**, 69 (1998).

¹³F. C. M. J. M. van, J. P. Weterings, A. K. van Langen-Suurling, and J. Romijn, *J. Vac. Sci. Technol. B* **18**, 3419 (2000).

¹⁴D. Thomas, G. Smith, and L. Nguyen, *Int. Dielectrics for ULSI Multilevel Interconnection Conference (DUMIC)* (1997), p. 361.

¹⁵H. Meynen, R. Uttecht, T. Gao, M. V. Hove, S. Vanhaelemeersch, and K. Maex, in *Low and High Dielectric Constant Materials*, edited by W. D. Brown, S. S. Ang, M. Loboda, S. Sammak, R. Singh, and H. S. Rathore (The Electrochemical Society Proceedings Series, Pennington, NJ, 1998), PV 98-3, p. 29.

¹⁶P. T. Liu, T. C. Chang, S. M. Sze, F. M. Pan, Y. J. Mei, W. F. Wu, M. S. Tsai, B. T. Dai, C. Y. Chang, F. Y. Shih, and H. D. Hung, *Thin Solid Films* **332**, 345 (1998).

¹⁷E. Kondoh, M. R. Baklanov, H. Bender, and K. Maex, *Electrochem. Solid-State Lett.* **1**, 224 (1998).